RESEARCH ARTICLE

WILEY Journal of RAMAN SPECTROSCOPY

Surface enhancement Raman spectroscopy and density functional theory study of silver nanoparticles synthetized with D-glucose

Alejandro González Fá[1,2] | Ignacio López-Corral[2,3] | Ricardo Faccio[4] | Alfredo Juan[1,5] | María Susana Di Nezio[2,3]

[1] Instituto de Física del Sur (IFISUR), UNS-CONICET, Bahía Blanca, Argentina

[2] Departamento de Química, Universidad Nacional del Sur, Bahía Blanca, Argentina

[3] Instituto de Química del Sur (INQUISUR), UNS-CONICET, Bahía Blanca, Argentina

[4] Centro NanoMat/CryssMat/Física, DETEMA, Facultad de Química, Universidad de la República, Montevideo, Uruguay

[5] Departamento de Física, Universidad Nacional del Sur, Bahía Blanca, Argentina

Correspondence

Alfredo Juan, Instituto de Física del Sur, Universidad Nacional del Sur-CONICET, Av. Alem 1253, Bahía Blanca 8000, Argentina.
Email: cajuan@uns.edu.ar

Abstract

The role of α- and β-D-glucose, and D-gluconate anion, acting as capping agent, on silver nanoparticles (AgNPs) was evaluated using both Raman and density functional theory studies. The particles were synthetized employing glucose, as reducing and blocking agent, in alkaline conditions. Capping agents were characterized through surface enhancement Raman spectroscopy together with modeling performed using silver clusters. Several geometries were optimized, and its energies and wavenumbers were calculated for each of them. Vibration normal modes from D-glucose isomers and D-gluconate were obtained and compared with those reported in bibliography, showing a satisfactory correlation. Comparison between experimental and calculated frequencies reveals a preference for D-gluconate anion acting as capping agent under the necessary presence of D-glucose on the surface of the AgNPs. The study of energies shows a greater affinity of D-gluconate for the silver atoms (above −1.3 eV for both geometries) than for other configurations of the glucose molecule (about −0.66 eV in the case of α-D-glucose).

KEYWORDS

capping agents, DFT, D-glucose, SERS, silver nanoparticles

1 | INTRODUCTION

Metal nanoparticles present remarkable optical and electronic properties. Its applications start from energy storage or water treatment to the development of catalysts and chemical sensors.[1] In the last years, with the aim to reduce the use of dangerous reagents, such as $NaBH_4$, new synthesis methods have been developed using natural reagents, such as glucose.[2] In all cases, silver nanoparticles (AgNPs), without capping agents, tend to agglomerate. These colloids can be stabilized according

to the following mechanisms: (a) electrostatics, (b) steric effect; (c) hydration forces, (d) depletion forces, and 5) van der Waals forces.[3] In almost all chemical synthesis process, the role of capping agents is fundamental to prevent the aggregation of nanoparticles (NPs).[4]

The efficiency of AgNPs is strongly related to the molecules adsorbed on their surface. An example of this is the different effect on its antibacterial properties that changes if the NPs are coated with monosaccharides (glucose or galactose) or disaccharides (maltose or lactose); the latter showed greater antibacterial effectiveness.[5] By other side,

shape, size, and Z potential were evaluated for different capping agents such as polyethylene glycol, ethylenediaminetetraacetic acid, polyvinyl pyrrolidone, and polyvinyl alcohol.[6] In the synthesis with honey or glucose solutions, this monosaccharide reacts with Ag^+ cations to produce Ag^0 and D-gluconate, in alkaline conditions. This anion can act as a stabilizing agent, together with the excess of α- and β-D-glucose present in the synthesis media.[7]

Raveendran et al. used a mixture of glucose with starch as reducing and capping agent.[2] For this synthesis, 20 hr of heating was necessary.[8] Other authors used mixtures of glucose with bamboo hemicellulose combined with the use of microwave.[8] A green synthesis, using common honey as both reducing and capping agent, was reported by our group.[9] We studied the roles of D-glucose and D-fructose to reduce the Ag^+ and their ability to act as a capping agent on AgNPs surface. Few works in bibliography identify the molecules that are responsible for stabilization of AgNPs during their synthesis,[10,11] whereas mainly adsorbed honey sugars and its preferential geometries on AgNPs are usually not studied in depth.

The surface enhancement Raman spectroscopy (SERS) is a phenomenon that greatly amplifies the intensity of vibration signal from molecules adsorbed to the surface of certain metals, such as Ag, when a green laser (532 nm) is used in Raman spectroscopy.[12,13] This technique can be used to find, through the SERS phenomenon, the normal modes from molecules linked to the AgNPs in colloidal suspension. Carlini et al. employed spin-resolved X-ray photoelectron spectroscopy and SERS to evaluate negatively charged hydrophilic organicthiol sodium 3-mercapto-1-propanesulfonate on AgNPs and gold nanoparticles (AuNPs).[14] On the other hand, Prado et al. analyzed the substitution of citrate by either thiocyanate or sulfide ions by changes in the normal vibration modes on the AuNPs surface.[15] Parameswari et al. used the SERS phenomenon to investigate the absorption of *N*-methylglycine and its orientation on the AgNPs surface and compared his measured data with density functional theory (DFT) computed wavenumbers.[16] The comparison between SERS and theoretical results for vibration normal modes is a strategy extensively used. Harrounhas carried out a thorough analysis of the adenine adsorption sites on gold and silver surfaces, using results obtained by different variants of Raman spectroscopy and computational calculation methods, finding that the experimental conditions are determinant in the nature of union of this molecule.[17] Using methodologies similar to those previously mentioned, Yao and Huang studied the possible conformations of absorption of cysteine on AuNPs, finding a preference in the interaction of this amino acid with the surface through its sulfur and oxygen atoms.[18] On the other hand, Maiti et al. measured the absorption of amino polycarboxylic acid

ligands on AgNPs using SERS and DFT methods. In this way, they found a strong chemisorption through oxygen and nitrogen atoms of the adsorbate with silver.[19]

In this work, we synthetize AgNPs using D-glucose and analyze different D-glucose/Ag and D-gluconate/Ag geometries using SERS and DFT methods in order to evaluate the role of these sugars as capping agent. This study is carried out by comparing the experimental vibrations with calculated normal modes, at the preferential adsorption configurations.

2 | METHODS

2.1 | Reagents

All reagents were of analytical grade. The water used was ultrapure (18 MΩ). Silver solution 5.88×10^{-3} mol L^{-1} was prepared by dissolving 0.0998 g of $AgNO_3$ (Merck 99.9%) in 100.0 ml in water. A 0.40 g of sodium hydroxide was diluted in 100.0 ml of water reaching 0.1 mol L^{-1} concentration. D-Glucose (Sigma-Aldrich) aqueous solution 78.20 g L^{-1} was prepared by dissolving 0.782 g of this sugar in 10.00 ml of water.

2.2 | Synthesis and characterization of AgNPs

A 40 μl of D-glucose solution was added to 265 μl of $AgNO_3$ solution (5.88×10^{-3} mol L^{-1}), and the pH 10.00 was adjusted with sodium hydroxide and diluted with water to a final volume of 10.0 mL. The colorless solution was stirred for 1 min. The appearance of typical brown-yellow color was observed, which indicates the formation of AgNPs.[9] Size and distribution of particles were obtained with a transmission electron microscope (JEOL 100 CX II).

2.3 | Raman measurements

For recording spectra of conventional Raman and SERS phenomena, the AgNPs suspension was deposited on a plate with aluminum (Al) bottom in a confocal Raman imaging Alpha 300R. The sample was irradiated for 2 min with a green laser ($Nd:Y_3Al_5O_{12}$) at 532 nm, and its power was kept at 10 mW. The integration time was 0.1 s.

2.4 | Computational details

A geometric optimization for isolated α- and β-D-glucose molecules and D-gluconate ion (Figure 1) was carried out in order to find their most stable configurations. We modeled AgNPs, using a cluster of three silver atoms (Ag_3), which was also optimized. This cluster has been used for several studies, including SERS spectra,
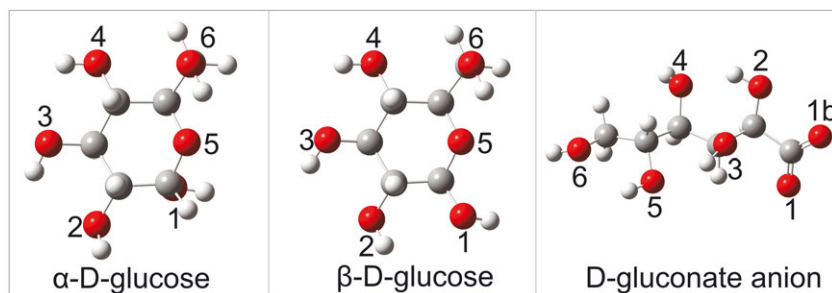
FIGURE 1 Structure of α-D-glucose, β-D-glucose, and D-gluconate anion, with the number of their corresponding oxygen atoms (in red). Carbon and hydrogen atoms are showed in gray and white color, respectively [Colour figure can be viewed at wileyonlinelibrary.com]

and proved to be a good model for AgNPs, leading to an excellent correlation between experimental and theoretical.[20–22] A total of 15 initial configurations were evaluated. Six of these configurations correspond to α-D-glucose: five of them interact with a closed triangular Ag$_3$ cluster, whereas the other one interacts with an open Ag$_3$ cluster. For the β-D-glucose, seven geometries were evaluated: five of them with the closed triangular Ag$_3$ cluster and two configurations with the open silver cluster. The D-gluconate anion was modeled through two

TABLE 1 Assignment of normal modes for D-glucose and D-gluconate

Experimental data/cm^{-1}	Literature data/cm^{-1}	Most probable assignment
531	515[33]	δ COO glu
	540[34]	δ C2–C1–O1 α
603	594[33]	δ CO + δ COO glu
662	651[33]	δ COO + δ COO glu
760	770[34]	δ O5–C1–O1 β
806	808[33]	δ CH glu
996	974[33]	υCO + δOCHglu
1,039	104[35]	δC1–H α
	1,039[33]	υCO α + δOCHglu
1,095	1,100[32]	υ CO + υ CC + δ COH α
	1,095[33]	υ CO + δ COO glu
1,108	1,112[32]	CC stretch + CCO bend α
1,176	1,150[36]	υ C–O endociclic gsa
1,209	1,202[33]	υ CO + δ COO glu
1,245	1,248[33]	δ COH + OCH glu
1,284	1,282[33]	δ OCH glu
1,307	1,310[33]	δ COH + δ OCH glu
1,339	1,349[35]	δ C–O–H α
	1,330[32]	ω CH2 α
	1,349[37]	δ COH + δ COH α
	1,336[36]	τ (CH2) gsa
	1,349[33]	δ COH + δ COH glu
1,363	1,360[34]	ω CH2 β
	1,368[38]	δ CH + δ OH gsa
	1,368[32]	ω CH2 + δ OCH + COH gsa
	1,349[33]	δ COH + δCOHglu
1,392	1,401[33]	υ COO-antisimetric glu
1,433	1,448[32]	δ CH2, OCH β
1,450	1,455[34]	δ CH2 gsa
	1,454[32]	CH2, δ OCH α
	1,445[33]	δ CH2 y OCH glu

Note. glu: D-gluconate; gse: D-glucose (isomer not specified); α: α-D-glucose; β: β-D-glucose.

configurations, all of them with the Ag$_3$ cluster in its closed triangular shape.

Calculations were carried out with the Gaussian 09 code, using the functional B3LYP. The basis set selected for C, O, and H atoms was 6-311 + G*, whereas the LANL2DZ basis set was used for Ag atoms.[23,24] The solvent effect was modeled using the implied hydration

instruction polarizable conductor calculation model (CPCM).[25,26]

For energies calculation, the following equation was used:

$$E_{ads} = E(\text{D-glucose}/\text{Ag}_3 \text{ or D-gluconate}/\text{Ag}_3) \\ - E(\text{Ag}_3) - E(\text{D-glucose or D-gluconate}), \quad (1)$$

TABLE 2 Initial and final adsorption geometries for α-D-glucose, β-D-glucose, and D-gluconate anion on Ag$_3$ cluster

Molecule	Initial interaction	Final interaction	Distance (Å) for final interaction	Energy (eV)
α-D-Glucose 1	O5 (ether)	O5 (ether)	2.52	−0.35
α-D-Glucose 2	O3; O4 (OH)	O3 (OH)	2.38	−0.49
α-D-Glucose 3	O2; O3; O4 (OH)	O3; O4 (OH)	3.51; 3.71	−0.08
α-D-Glucose 3 (with open Ag$_3$)	O2; O3; O4 (OH)	O1; O2 (OH)	2.85; 2.67	−0.30
α-D-Glucose 4	O1; O2 (OH)	O1; O2 (OH)	2.57; 2.53	−0.66
α-D-Glucose 5	O2; O3 (OH)	O1; O2 (OH)	2.78; 2.46	−0.48
β-D-Glucose 1	O5 (ether)	O1 (OH); O5 (ether)	2.56; 2.72	−0.62
β-D-Glucose 2	O3; O4 (OH)	O4 (OH)	3.57	−0.05
β-D-Glucose 2 (with open Ag$_3$)	O3; O4 (OH)	O6 (hydroxymethyl)	2.50	−0.24
β-D-Glucose 3	O2; O3; O4 (OH)	O4 (OH)	2.42	−0.40
β-D-Glucose 4	O1; O2 (OH)	O1 (OH)	2.44	−0.43
β-D-Glucose 5	O2; O3 (OH)	O2; O3 (OH)	3.69; 3.66	−0.07
β-D-Glucose 5 (with open Ag$_3$)	O2; O3 (OH)	O3 (OH)	3.66	−0.04
D-Gluconate 1	O1; O1b (carbonyl group)	O1 (carbonyl group)	2.25	−1.93
D-Gluconate 2	O2; O3; O4 (OH)	O2; O3 (OH)	2.68; 2.43	−1.32

Note. The final adsorbate/cluster distance and adsorption energy value are indicated for each system.

FIGURE 2 Final adsorption geometries for the α-D-glucose/Ag$_3$ system: (a) Geometry 1 (α-1); (b) Geometry 2 (α-2); (c) Geometry 3 (α-3); (d) Geometry 4 (α-4); (e) Geometry 5 (α-5); and (f) Geometry 3 with Ag$_3$ open cluster (3-α-O). Oxygen, carbon, and hydrogen atoms are shown in red, gray, and white, respectively, whereas light blue atoms corresponds to the silver cluster [Colour figure can be viewed at wileyonlinelibrary.com]
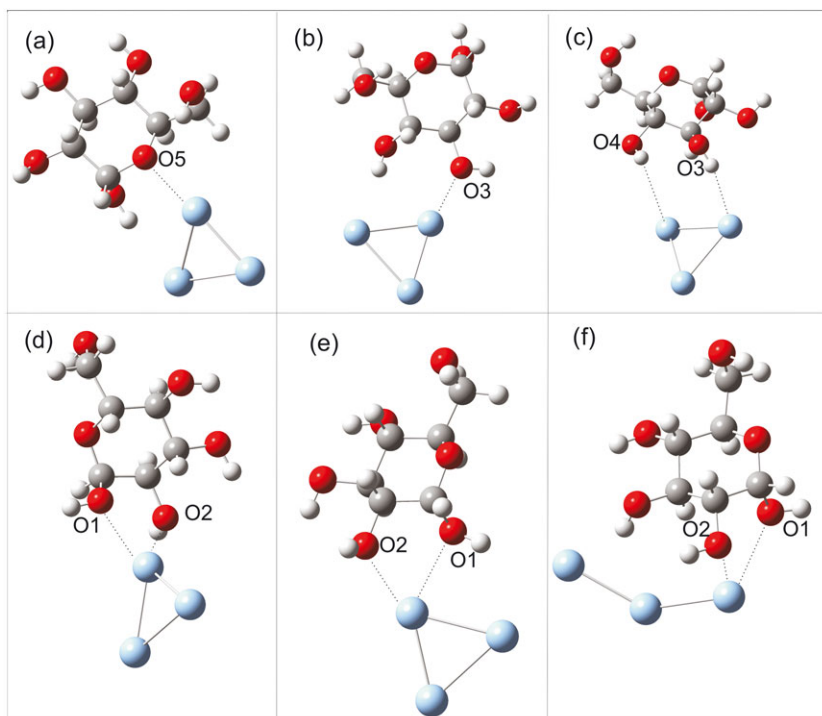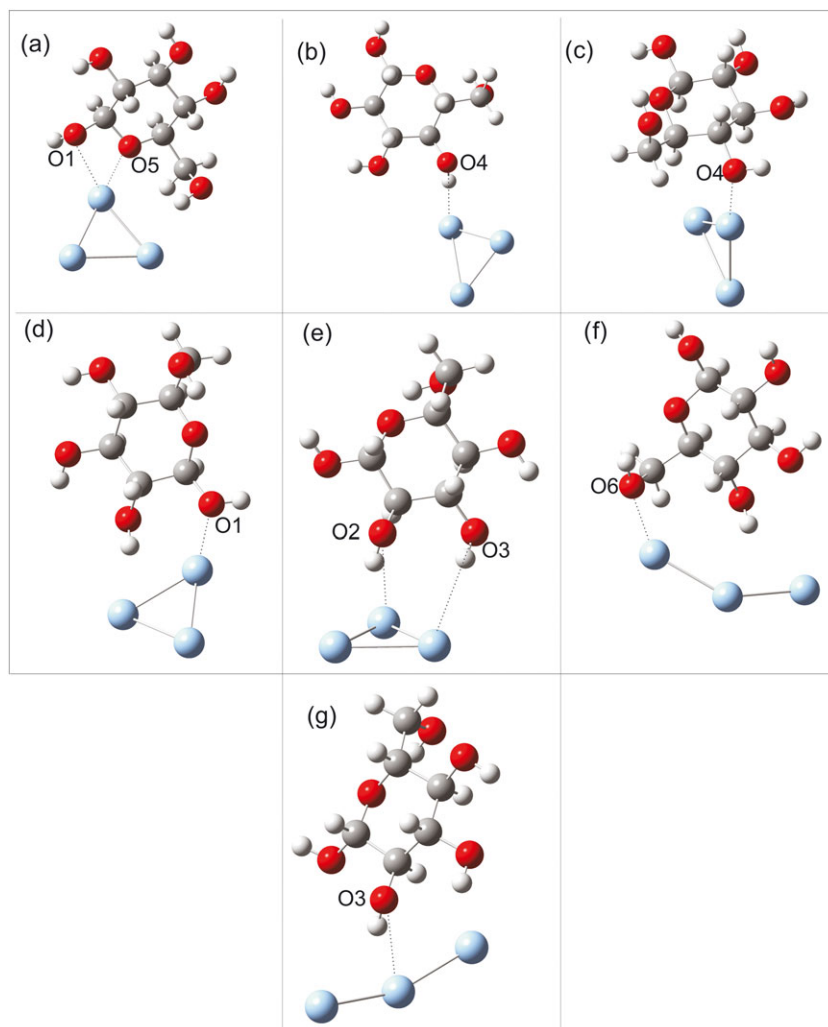
FIGURE 3 Initial and final adsorption geometries for the β-D-glucose/Ag$_3$ system: (a) Geometry 1 (β-1); (b) Geometry 2 (β-2); (c) Geometry 3 (β-3); (d) Geometry 4 (β-4); (e) Geometry 5-β; (f) Geometry 2 with Ag$_3$ open cluster (β-2-O); and (g) Geometry 5 with Ag$_3$ open cluster (β-5-O). Oxygen, carbon, and hydrogen atoms are shown in red, gray, and white, respectively, whereas light blue atoms correspond to the silver cluster [Colour figure can be viewed at wileyonlinelibrary.com]

where E (D-glucose or D-gluconate/Ag$_3$) represents the energy of adsorbed molecules on the Ag$_3$ cluster, E (Ag$_3$) the energy of isolated silver cluster, and E (D-glucose or D-gluconate) the energy of isolated molecule.

A basis set superposition error correction, a consequence of inconsistent treatment of complex system and its constituent subsystems, present especially in transition metals, was also made.[27,28]

3 | RESULTS AND DISCUSSION

3.1 | Synthesis of AgNPs

The synthesized AgNPs showed spherical, polyhedral, and nanoprism shapes. Particle size shows a binomial distribution with an average of 25 and 45 nm, which can be observed in Figure S1. Similar characteristics were revealed in González Fá et al.[9]
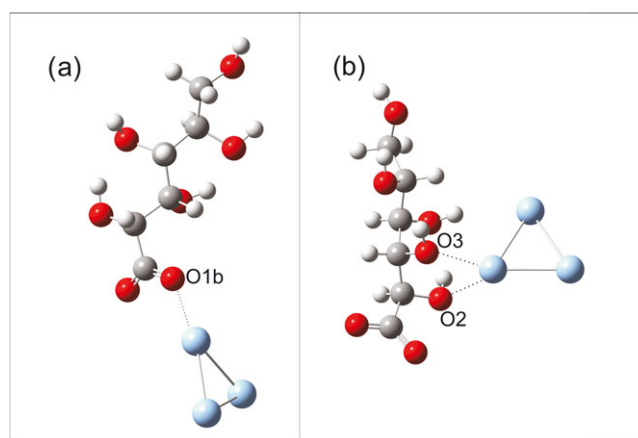

FIGURE 4 Initial and final adsorption geometries for the D-gluconate/Ag$_3$ system: (a) Geometry 1 (Glu-1) and (b) Geometry 2 (Glu-2). Oxygen, carbon, and hydrogen atoms are shown in red, gray, and white, respectively, whereas light blue atoms correspond to the silver cluster [Colour figure can be viewed at wileyonlinelibrary.com]

3.2 | Raman spectroscopy of solid α-D-glucose

In order to check the possibility of comparing experimental normal modes with bibliography data, a conventional Raman spectrum of α-D-glucose powder was obtained, and its wavenumbers were compared. Table S1 present an excellent correlation (see also Figure S2), considering that the experimental error is ± 10 cm^{-1}.

3.3 | Surface enhancement Raman spectroscopy

In all the cases, the obtained peaks can be assigned to the glucose molecule or the D-gluconate anion adsorbed on the silver surface; this is because the free molecules are not close enough to give the SERS phenomenon. These wavenumbers were compared with those reported in bibliography for D-glucose molecule and D-gluconate ion

measurements, in order to make the corresponding assignments of the normal vibration modes (see Table 1).

Wavenumbers shown in Table 1 suggest α-D-glucose, β-D-glucose, and also D-gluconate anion are adsorbed on the silver surface of the AgNPs, because the wavenumbers present in the experiments correspond to those found in literature for these species.[29–35] Small discrepancies are observed and can be attributed to the different concentration of the carbohydrate present in the sample with respect to that used in literature.[29–35] In the present work, the initial concentration of α-D-glucose in the synthesis was 0.0345% (w/v), whereas in the literature, the concentration of the monosaccharides was higher than 20% (w/v).[27,29,31–35] High concentration of D-glucose can lead to interactions by the solute molecules through van der Waals forces or hydrogen bonds, producing changes in the Raman shift.[36] Moreover, the wavenumbers obtained experimentally were carried out in an alkaline medium (pH 10.00), whereas the measurement of normal modes obtained from the literature was

TABLE 3 Matching of experimental and theoretical wavenumbers

| Experimental wavenumbers | Theoretical wavenumbers for final adsorption geometries (cm^{-1}) | | | | | | | | | | | | | | |
| | α-D-Glucose/Ag$_3$ | | | | | | β-D-Glucose/Ag$_3$ | | | | | | | D-Gluconate/Ag$_3$ | |
	α-1	α-2	α-3	α-3-O	α-4	α-5	β-1	β-2	β-2-O	β-3	β-4	β-5	β-5-O	Glu 1	Glu 2
531			536	539	537	537									539
603							606	605	605	605	608	607	605		
662		672													
760														757	766
806															*823*
996				1,003	993	990	998	1,001	999	999	997	990	996		
1,039	1,039	1,042	1,033	1,035	1,040	1,044	1,033	1,045	1,048		1,033	1,032	1,032	1,038	1,045
1,095				1,096	1,091	1,097	1,097	1,106						1,090	1,094
1,108	1,110	1,104	1,098						1,108	1,109		1,108	1,110		
1,176	1,170	1,171	1,181	1,182	1,181	1,184				1,172				1,175	1,186
1,209	1,206	1,209	1,205	1,211	1,211	1,205	1,210	1,211	1,205	1,209	1,206	1,208	1,207	1,207	1,205
1,245															1,254
1,284	1,292	1,285			1,292	1,290	1,289	1,289	1,289	1,293	1,286	1,280	1,285		1,280
1,307	1,305	1,304	1,308	1,304	1,305	1,303	1,306	1,310	1,309	1,311	1,303	1,312	1,304	1,305	1,314
1,339	1,336	1,346	1,339	1,339	1,337	1,338	1,343	1,345	1,344	1,348	1,342	1,337	1,341	1,338	1,343
1,363		1,367		1,370	1,372			1,371	1,371	1,356				1,370	1,365
1,392	1,394	1,383	1,392	1,396	1,391	1,391	1,395	1,388	1,386	1,397	1,394	1,389	1,396	1,390	1,391
1,433							1,436					1,429			
1,450	1,449	1,445	1,445	1,444	1,443	1,445		1,444	1,445	1,445	1,444	1,445	1,446	1,460	
1,548															1,552
1,567														1,563	

Note. Instrument error is ± 10 cm^{-1}. The wavenumbers in italics exceed the difference ± 10 cm^{-1} (instrument error).

α: alpha-D-glucose; β: beta-D-glucose; Glu: D-gluconate; O: interaction with open Ag$_3$ cluster.

done in distilled water.[26–32] On the other hand, there is evidence about a slight shift in wavenumbers between conventional Raman measurements and SERS.[37,38] It should be noted that the wavenumbers found in literature for the D-gluconate anion are in solid state, leading to possible differences.[30]

3.4 | Computational simulation

Table 2 shows the different interactions between the Ag₃ cluster with D-glucose molecule and the D-gluconate anion. The initial proposed interactions geometries for these molecules are also shown. The final adsorption configurations are shown in Figures 2 (α-D-glucose), 3 (β-D-glucose), and 4 (D-gluconate anion), and in each case, it can be observed the evolution to a more stable configuration. The theoretical Raman wavenumbers belong to these final adsorption geometries. On the other hand, Table 2 also presents information about the adsorption energy for each final configuration, calculated with Equation 1, so the preferential adsorption geometries could be recognized.

The obtained configurations, at their most stable form, after geometric optimization are showed in figure 2, 3 and 4.

We also analyze adsorption geometries with an open Ag₃ cluster (see Table 2 and Figures 2, 3, and 4). This is due to the distance between the oxygen and silver atoms, which is always greater than 3 Å when the cluster is in closed triangular form, so in these cases, the adsorbate–Ag₃ interaction is very weak, and another configuration for the cluster should also be considered. On the other hand, the adsorption energy values were more negative in the case of the Ag₃ open form, except for the Geometry 5 of β-D-glucose (β-5), where no significant changes were found. Table 2 also shows that most interactions between α-D-glucose and the Ag₃ cluster involve O1 and O2 atoms, but this situation does not repeat with the β-D-glucose. A different position occupied by O1 atom in this isomer could be the reason.

After analysis of the adsorption energy values from Table 2, the adsorbates could be organized into three groups according to their stability. The most stable molecule is the D-gluconate anion, mainly its (see Geometry 1, Figure 4a), with an adsorption energy value of −1.93 eV, followed by its Geometry 2 with an energy value of −1.32 eV. In a second group, no significant differences in energy are found between the D-glucose isomers, being the most stable, for α-D-glucose, the Configurations 4, 2, and 5 with adsorption energy values of −0.66, −0.49, and −0.48 eV, respectively, and for the β-D-glucose, Geometries 1, 4, and 3 with energy values of −0.62, −0.43, and −0.40 eV, respectively. Finally, in a third

group, the open Ag₃ shows less stability when it interacts with Geometries 1 and 3 of α-D-glucose (with energy values of −0.35 and − 0.30 eV, respectively) and Configuration 2 of β-D-glucose −0.24. Geometry 3 of α-D-glucose (with closed triangular Ag₃ cluster) and Configuration 5 of the β-isomer (with open and closed triangular Ag₃ clusters) are virtually non-interacting (see Figures 2 and 3).

3.5 | Theoretical–experimental vibrational analysis

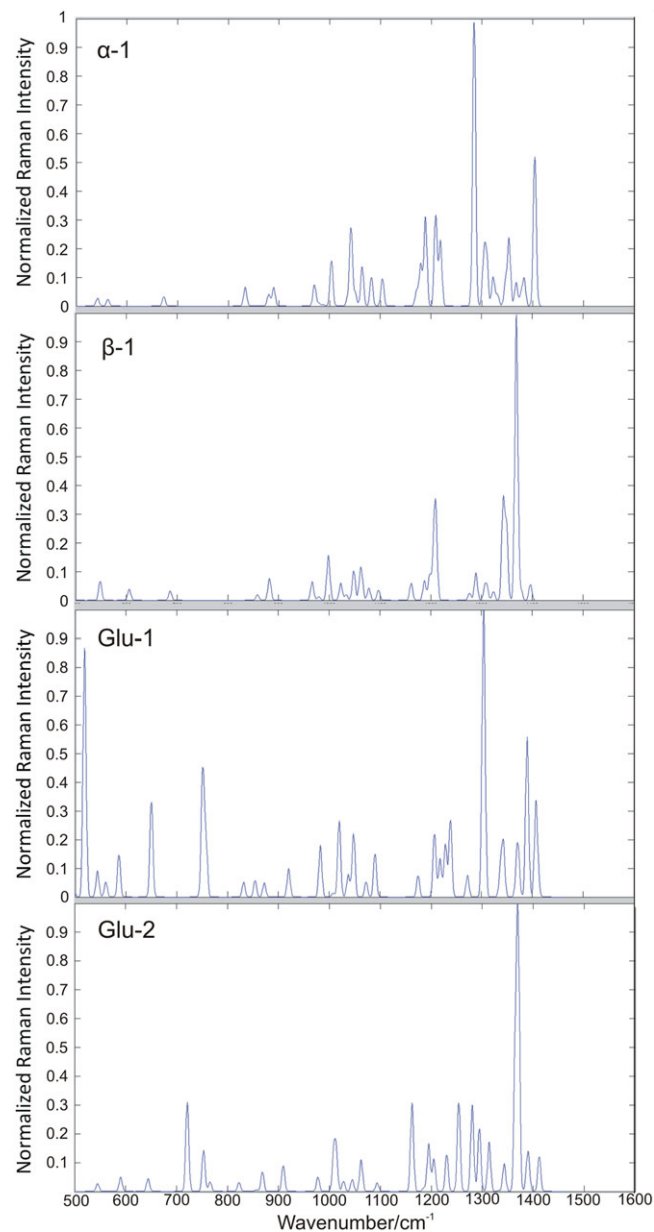Table 3 lists the theoretical and experimental wavenumbers belonging to α-D-glucose, β-D-glucose, and

FIGURE 5 Theoretical Raman spectra for the most probable geometries [Colour figure can be viewed at wileyonlinelibrary.com]
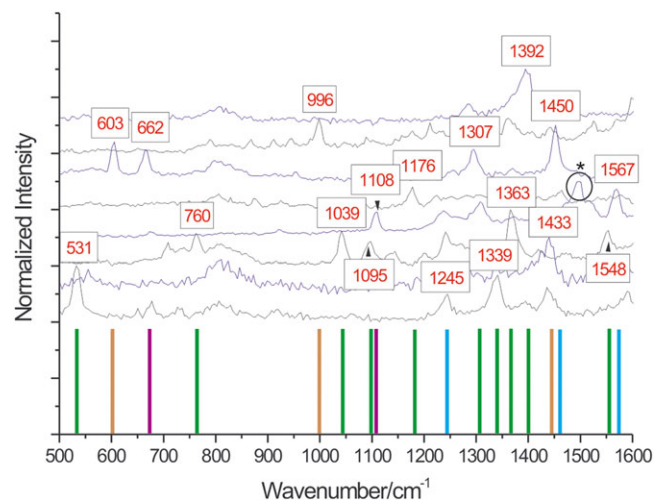
FIGURE 6 Schematic representation of theoretical and experimental wavenumbers (upper part). Bars represent the calculated normal modes (lower part). Blue: D-gluconate geometry 1 (Glu 1); green: D-gluconate geometry 2 (Glu 2); violet: α-D-glucose geometry 2 (α-2); brown: β-D-glucose geometry 1 (β-1). *Frequency not found in literature or calculation [Colour figure can be viewed at wileyonlinelibrary.com]

D-gluconate on AgNPs, which are compared in order to infer the adsorption geometries that are most plausible to be adsorbed on silver clusters.

In Figure 5, theoretical vibrational spectra for the most probable geometries are presented with its respective normalized Raman intensities.

As can be seen, the experimental wavenumbers at 760 and 1,567 cm^{-1} only appear in Geometry 1 of D-gluconate (Glu 1), whereas the vibrations in 806, 1,133, and 1,548 cm^{-1} are only present Geometry 2 of this anion (Glu 2). These two configurations involve almost all the experimental observed wavenumbers, except 603, 662, 996, 1,108, and 1,433 cm^{-1}. On the other hand, the vibration at 662 cm^{-1} is only present in Geometry 2 of α-D-glucose (α-2), making this configuration highly probable. This configuration also contributes to the vibration at 1,108 cm^{-1}. The remaining normal modes can be found in Geometries 1 and 5 of β-D-glucose (β-1 and β-5), making these configurations preferable over the other β-D-glucose/Ag$_3$ systems evaluated. Figure 6 shows a schematic representation of experimental and theoretical matching for measured and calculated wavenumbers.

4 | CONCLUSIONS

In this work, an experimental and theoretical analysis of capping agents on AgNPs synthesized with glucose was studied by SERS and DFT. We have found good correlations between our experimentally obtained vibrational

wavenumbers and those reported in literature. Correlation between experimental and calculated wavenumbers indicates that both D-glucose and D-gluconate adsorption geometries can be found on the silver surface. These results suggest that the utilized silver cluster may be considered a satisfactory approximation for AgNPs. However, the calculations show that the D-gluconate anion becomes essential to assign many wavenumbers found experimentally. This also applies to Geometry 2 of α-D-glucose and Geometry 1 or 5 of β-D-glucose, although the latter has a very low adsorption energy value; being therefore more probable to find Geometry 1. Therefore, the studies would indicate that D-gluconate anion can be found as a capping agent and then the glucose molecules in their Configurations 2 of α-D-glucose and 1 of β-D-glucose. It is also found that the interaction point between silver and α-D-glucose tends to occur preferentially through O1 and O2 oxygen atoms. This does not seem to occur in β-D-glucose, probably because these atoms are in different positions due to the isomerism. In this way, the proposed strategy allows corroborate that both glucose and its oxidation product (D-gluconate anion in alkali medium) are present on the surface of the AgNPs and also make inferences about most probable geometries and preferential points of union.

ORCID

Alejandro González Fá 🔴 http://orcid.org/0000-0002-7878-658X
Ricardo Faccio 🔴 http://orcid.org/0000-0003-1650-7677

REFERENCES

[1] T. Maiyalagan, *Appl. Catal. Gen.* **2008**, *340*, 191.

[2] P. Raveendran, J. Fu, S. L. Wallen, *J. Am. Chem. Soc.* **2003**, *125*, 13940.

[3] K. Do Kim, D. N. Han, H. T. Kim, *Chem. Eng. J.* **2004**, *104*, 55.

[4] A. B. Smetana, K. J. Klabunde, C. M. Sorensen, J. Colloid Interface, *Forensic Sci.* **2005**, *284*, 521.

[5] L. Kᴠɪ, R. Vec, *J. Phys. Chem. B* **2006**, *110*, 16248.

[6] B. Ajitha, Y. A. Kumar Reddy, P. S. Reddy, H.-J. Jeon, C. W. Ahn, *RSC Adv.* **2016**, *6*, 36171.

[7] X. Sun, C. Zheng, F. Zhang, Y. Yang, G. Wu, A. Yu, N. Guan, *J. Phys. Chem. C* **2009**, *113*, 16002.

[8] H. Peng, A. Yang, J. Xiong, *Carbohydr. Polym.* **2013**, *91*, 348.

[9] A. J. González Fá, A. Juan, M. S. Di Nezio, *Ann. Lett.* **2016**, *50*, 877.

[10] M. N. Siddiqui, H. H. Redhwi, D. S. Achilias, E. Kosmidou, E. Vakalopoulou, M. D. Ioannidou, *J. Polym. Environ.* **2018**, *26*, 423.

[11] M. Hosseini, F. Mehrabi, M. R. Ganjali, P. Norouzi, *Adv. Nat. Sci. Nanosci. Nanotechnol.* **2017**, *8*, 1339.

[12] M. Kahraman, E. R. Mullen, A. Korkmaz, S. Wachsmann-Hogiu, *Nanomedicine* **2017**, *6*, 831.

[13] E. Smith, G. Dent, *Modern Raman Spectroscopy–A Practical Approach*, John Wiley & Sons Ltd, Southern Gate, Chichester, West Sussex **2005**.

[14] L. Carlini, C. Fasolato, P. Postorino, I. Fratoddi, I. Venditti, G. Testa, C. Battocchio, *Colloids Surf. A Physicochem. Eng. Asp.* **2017**, *532*, 183.

[15] A. R. Prado, D. O. de Souza, J. P. Oliveira, R. H. A. Pereira, M. C. C. Guimarães, B. V. Nogueira, P. V. Dixini, M. R. N. Ribeiro, M. J. Pontes, *Appl. Spectrosc.* **2670**, *2017*, 71.

[16] A. Parameswari, R. M. Asath, R. Premkumar, A. M. F. Benial, *J. Mol. Struct.* **2017**, *1138*, 102.

[17] S. G. Harroun, *Chemphyschem* **2018**, *19*, 1003. https://doi.org/10.1002/cphc.201701223

[18] G. Yao, Q. Huang, *J. Phys. Chem. C* **2018**, *122*, 15241. https://doi.org/10.1021/acs.jpcc.8b00949

[19] N. Maiti, V. V. Malkar, T. Mukherjee, S. Kapoor, *J. Mol. Struct.* **2018**, *1156*, 592.

[20] T. N. Rekha, B. J. M. Rajkumar, *Can. J. Phys.* **2015**, *8*, 1.

[21] U. Reeta Felscia, B. J. M. Rajkumar, P. Sankar, R. Philip, M. Briget Mary, *Spectrochim. Acta - Part a Mol. Biomol. Spectrosc* **2017**, *184*, 286.

[22] U. R. Felscia, B. J. M. Rajkumar, M. Nidya, P. Sankar, *J. Phys. Chem. A* **2018**, *122*, 1045.

[23] P. J. Hay, W. R. Wadt, *J. Chem. Phys.* **1985**, *82*, 299.

[24] L. E. Roy, P. J. Hay, R. L. Martin, L. E. Roy, P. J. Hay, R. L. Martin, *J. Chem. Theory Comput.* **2008**, *4*, 1029.

[25] V. Barone, M. Cossi, *J. Phys. Chem. A* **2001**, *102*, 1995.

[26] M. Cossi, N. Rega, G. Scalmani, V. Barone, *J. Comput. Chem.* **2003**, *24*, 669.

[27] S. Simon, M. Duran, J. J. Dannenberg, *J. Chem. Phys.* **1996**, *105*, 11024.

[28] S. F. Boys, F. Bernardi, *Mol. PHYSIC.* **1970**, *19*, 553.

[29] E. C. Corbett, V. Zichy, J. Goral, C. Passingham, *Spectrochim. Acta Part a Mol. Spectrosc.* **1991**, *47*, 1399.

[30] H. A. Tajmir-Riahi, J. T. Agbebavi, *Carbohydr. Res.* **1993**, *241*, 25.

[31] M. Mathlouthi, D. VinhLuu, *Carbohydr. Res.* **1980**, *81*, 203.

[32] P. D. Vasko, J. Blackwell, J. L. Koenig, *Carbohydr. Res.* **1972**, *23*, 407.

[33] M. Kačuráková, M. Mathlouthi, *Carbohydr. Res.* **1996**, *284*, 145.

[34] A. N. Batsoulis, N. G. Siatis, A. C. Kimbaris, E. K. Alissandrakis, C. S. Pappas, P. A. Tarantilis, P. C. Harizanis, M. G. Polissiou, *J. Agric. Food Chem.* **2005**, *53*, 207.

[35] R. Goodacre, B. S. Radovic, E. Anklam, *Appl. Spectrosc.* **2002**, *56*, 521.

[36] S. Datta, K. Kumar, *Spectrochim. Acta - Part A Mol. Biomol. Spectrosc* **2006**, *64*, 665.

[37] A. E. Aliaga, C. Garrido, P. Leyton, G. Diaz, J. S. Gomez-Jeria, T. Aguayo, E. Clavijo, M. M. Campos-Vallette, S. Sanchez-Cortes, *Spectrochim. Acta - Part A Mol. Biomol. Spectrosc* **2010**, *76*, 458.

[38] C. Garrido, T. Aguayo, E. Clavijo, J. S. Gõmez-Jeria, M. M. Campos-Vallette, *J. RamanSpectrosc.* **2013**, *44*, 1105.

SUPPORTING INFORMATION

Additional supporting information may be found online in the Supporting Information section at the end of the article.